Magnetoresistance effects in laterally confined n-GaAs/(AlGa)As heterostructures

1989 J. Phys.: Condens. Matter 1 10413

(http://iopscience.iop.org/0953-8984/1/51/014)

J. Phys.: Condens. Matter 1 (1989) 10413–10425. Printed in the UK

Magnetoresistance effects in laterally confined n-GaAs/(AlGa)As heterostructures

R P Taylor†, P C Main†, L Eaves†, S P Beaumont‡, I McIntyre‡, S Thoms‡ and C D W Wilkinson‡

† Department of Physics, University of Nottingham, Nottingham NG7 2RD, UK
‡ Department of Electronics and Electrical Engineering, University of Glasgow, Glasgow GL2 5QQ, UK

Received 15 May 1989

Abstract. We have investigated the magnetoresistance of laterally confined n-GaAs/(AlGa)As heterostructures in the temperature range from 2 K to 300 K and at magnetic fields up to 11 T. The 2DEG at the interface is confined to narrow channels which are 10 μm long and with lithographic widths between 0.16 μm and 0.54 μm. We assess the effectiveness of the confinement in terms of carrier depletion, the nature of the side-wall scattering and the stability of the conductivity as a function of time. We also compare the conduction channel width with the lithographic width. The low field magnetoresistance is analysed in terms of electron interaction effects, weak localisation, universal conductance fluctuations (UCF) and a side-wall skipping orbit effect. In particular, at high temperatures ($T > 20$ K) the skipping effect develops a temperature dependence which is explained by the variation of the phase-breaking rate obtained from the UCF analysis.

1. Introduction

The two-dimensional electron gas (2DEG) is an excellent system for the study of low dimensional transport phenomena. The silicon MOSFET has proved particularly useful due to the ease with which the carrier density can be controlled by means of a gate voltage. However, higher electron mobilities are achieved in the modulation doped $(Al_xGa_{1-x})As/GaAs$ heterostructure system, principally due to the spatial separation of the ionised impurities from the conducting electrons in the 2DEG. With recent advances in fabrication techniques [1], it is now possible to confine laterally such a 2DEG to a conducting channel with a width smaller than the elastic mean free path l. In such a case, the electrons are in the 'quasi-ballistic' regime ($W < l < L$ where W and L are the channel width and length respectively). The existing theories based on the diffusive models for the 'dirty metal' regime [2] require modification to explain the various magnetoresistance effects associated with the quasi-one-dimensional character of these systems.

In this paper, magnetoresistance measurements taken between 4.2 and 48 K on channels of length 10 μm and physical widths of 0.16–0.54 μm are described in terms of the available theories for the quasi-ballistic regime. We will show that, in addition to giving an insight into the electronic behaviour of the system, the measurements also provide information about the effectiveness of the fabrication technique used to confine

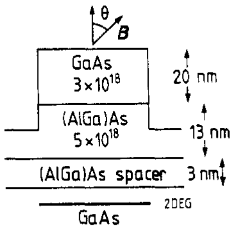

Figure 1. Schematic cross-section of the structure (doping levels are in cm^{-3}).

the 2DEG laterally. In particular, the nature of the side-wall scattering process can be determined, as can the extent of the depletion of the carrier concentration. It is also possible to extract the conduction channel width W, which may differ from the lithographic width. Finally, this information will be used to study the slow decrease in the conductivity with time observed in the narrower structures when they are held at cryogenic temperatures for several days.

A schematic cross-sectional diagram of the structure, grown using molecular beam epitaxy, is shown in figure 1 and includes the Si doping levels in the two top layers. The Al composition is 33%. The carrier concentration of the bulk material is 6.2×10^{15} m^{-2} with a mobility, μ, of 4.7 $m^2\,V^{-1}\,s^{-1}$. The fabrication technique, involving electron beam lithography and $SiCl_4$ dry etching [1], is referred to as 'shallow etch confinement' since the lateral confinement of the 2DEG is achieved without the removal of the entire (AlGa)As layer. In this way the effect of the surface damage on the 2DEG is reduced, as is the side-wall depletion. Alternative confinement techniques are deep etching, where the entire (AlGa)As layer is etched (for example [3, 4]), and the use of an electric field from a split gate at the surface [5, 6]. Both of these techniques give a conducting width which is considerably less than the physical width. We will show that using the shallow etch technique the two widths are approximately the same.

2. Characteristic length scales of the system

The quantisation of energy levels due to confinement of the electronic motion in the width direction is prevented by the collision broadening of the levels. For example, for a channel of width $W = 0.32$ μm the broadening at 4.2 K approximately equals the energy separation between the lowest two levels ($\approx\frac{1}{2}$ meV). Hence the channels are not one-dimensional in terms of sub-band formation and the two-dimensional expressions for the diffusion coefficient and the density of states have to be used. However, we will show that the channels do exhibit quasi-one-dimensional behaviour in respect to weak localisation, universal conductance fluctuations and electron interaction effects. The effective dimensionality of the channel depends upon the electronic process under study since each effect is governed by a different characteristic length scale. The six length scales considered in this paper are summarised in table 1. It is necessary to distinguish between two scattering times. The transport scattering time τ_t is related to the DC conductivity σ_0 by

$$\sigma_0 = n_s e^2 \tau_t / m^* \tag{1}$$

where $m^* = 0.067m_e$ is the effective mass and n_s is the carrier concentration. The carrier

Table 1. Summary of various characteristic length scales. D is the diffusion coefficient, k_F is the Fermi wavevector and v_F is the Fermi velocity.

Phase coherence length	$L_\varphi = (D\tau_\varphi)^{1/2}$	Fermi wavelength	$\lambda_F = 2\pi/k_F$
Thermal diffusion length	$L_T = (\hbar D/k_B T)^{1/2}$	Magnetic length	$L_B = (\hbar/eB)^{1/2}$
Cyclotron radius	$L_c = \hbar k_F/eB$	Elastic mean free path	$l = v_F\tau_t$

lifetime, τ_c, is a measure of the time for which the electronic momentum eigenstate can be defined in the presence of scattering. Consider the elastic components of the rates τ_c^{-1} and τ_t^{-1}, each of which is related to a corresponding length by the Fermi velocity v_F. The two rates are equal for short range scattering events where the cross-section is independent of angle. However, for scattering processes which are strongly peaked in the forward direction, τ_t can become much larger than τ_c [7]. In particular, this is true for Coulombic scattering due to remote ionised impurities in the (AlGa)As layer, where for a structure similar to ours, a ratio of $\tau_t/\tau_c \simeq 30$ has been calculated [7]. However, the results of Lakrimi *et al* [4] suggest that in the field range 0–1 T the electronic motion in our channels will be dominated by short range scatterers within the channel itself, resulting in a ratio close to unity. The work of Lakrimi *et al* was carried out on very wide channels ($W = 22\ \mu$m). For our narrower channels, scattering off the side walls will also play an important role. If the side-wall scattering were totally specular, τ_t would be insensitive to such a scattering process, whilst τ_c would be altered considerably. However, if this scattering is diffuse in nature then the ratio of the two times will be unaffected (i.e. $\tau_t/\tau_c \approx 1$). In this way, the ratio of the two times will be used to explore the nature of the side-wall scattering.

3. Magnetoresistance measurements

Figure 2 shows magnetoresistance measurements taken at temperatures from 4.2 K to 105 K by applying a small magnetic field perpendicular to a 2DEG plane confined to a channel of lithographic width 0.32 μm. In order to explain the trends shown in these traces, it is necessary to consider three electronic processes, each of which results in a small correction to the Drude conductivity. Since the corrections are small, the behaviour of the system can be explained by adding the resistance due to the three effects.

3.1. Quantum interference effects

The small reproducible resistance variations, seen on top of the background resistance, arise from quantum interference (QI) between pairs of partial wavefunctions of the same electron travelling along different trajectories within the channel. There are two types of interference process. For indirect interference, one partial wave represents the possibility of an electron traversing a closed path or loop formed by scatterers. The second wave represents the possibility of traversing the same loop in the opposite direction. On arriving back at the origin, the two waves interfere. For direct interference the two partial waves interfere at sites other than the origin. In both cases the interference pattern is sensitive to the magnetic flux threaded through the area enclosed, resulting in a variation of resistance with B. Indirect interference processes result in a phenomenon called weak localisation, WL, whilst direct interference is widely used to explain universal

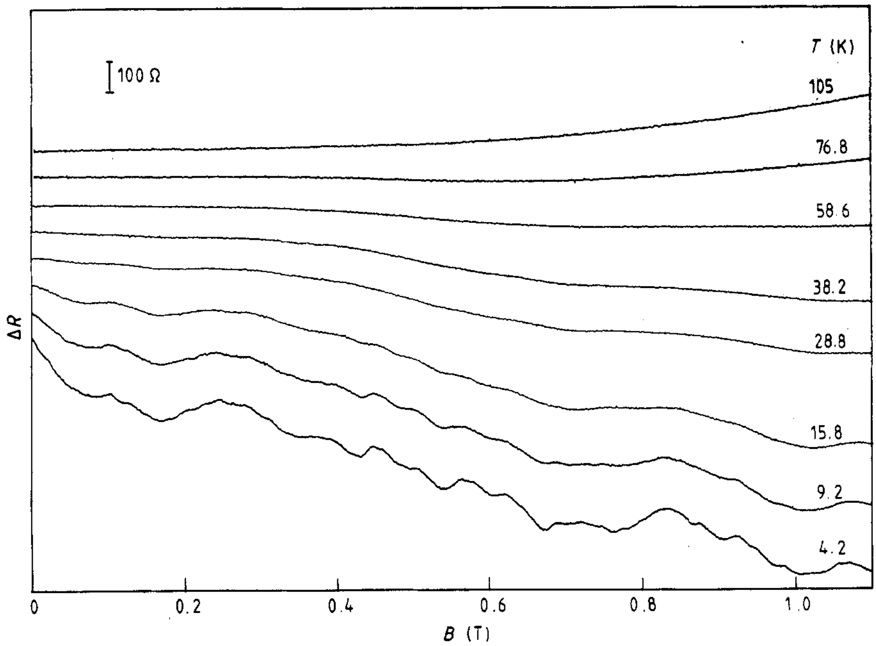

Figure 2. Magnetoresistance of a 0.32 μm wide structure at different temperatures. The traces are displaced for clarity. The zero-field resistance values are as follows: 9.45 (bottom), 9.18, 8.98, 8.75, 8.68, 9.21 and 10.55 (top) kΩ.

conductance fluctuations (UCF). The sharp negative magnetoresistance below 0.1 T is attributed to WL. Other workers have derived equations for the WL effect in the quasi-ballistic regime [8], though a detailed analysis is not carried out here due to the distorting effects of the UCF. Note, however, that we expect the fall-off to be a one-dimensional WL effect since the 2D WL effect is predicted to saturate when the magnetic length L_B becomes comparable to or smaller than the elastic scattering length, which occurs for $B > 0.01$ T in these channels.

The UCF can be quantified by the variance of the fluctuation amplitude, which is affected by the side walls only implicitly through the diffusion coefficient. The dimensionality of the channel is determined by L_φ and L_T. For a one-dimensional channel ($W < L_\varphi$, $L_T < L$) at finite temperatures, the following expressions are true for the variance S^2 [9]

$$S^2 = \alpha^2(e^2/h)^2(L_\varphi/L)^3 \qquad \text{if } L_\varphi \ll L_T \tag{2}$$

and

$$S^2 = \beta^2(e^2/h)^2(L_T^2 L_\varphi/L^3) \qquad \text{if } L_\varphi \gg L_T \tag{3}$$

where α and β are numerical coefficients with values close to unity. These expressions are valid only in the limits stated. Results for other regimes can be found in Lee *et al* [9]. The interpretation of these equations to extract L_φ varies in the literature and here we consider methods followed by Beenakker *et al* [10] and Thornton *et al* [5] who obtain L_φ for structures similar to ours. For a sample geometry similar to ours Beenakker calculates

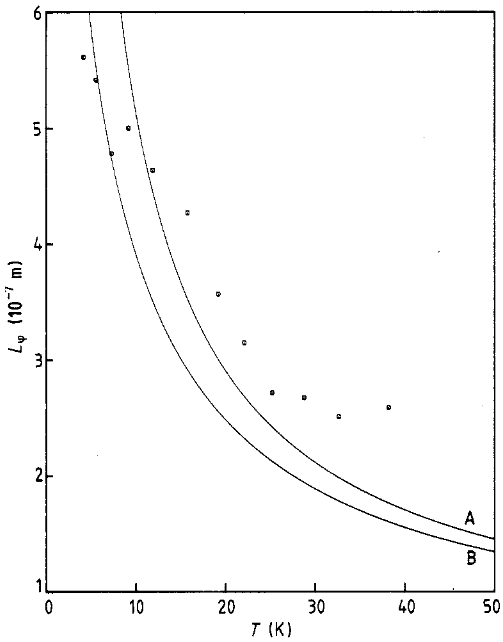

Figure 3. L_φ against T. The curves show fits to (A) equation (5*a*), (B) the combined rate.

$\alpha = \sqrt{6}$ and $\beta = \sqrt{4\pi/3}$ and also notes that, since L_φ and L_T are comparable, it is necessary to interpolate between equations (2) and (3), giving

$$S^2 = 6(e^2/h)^2(L_\varphi/L)^3[1 + (9/2\pi)(L_\varphi/L_T)^2]^{-1}. \tag{4}$$

Using this approach we find for $T = 4.2$ to 38 K that L_φ decreases from 0.27 to 0.13 μm. Thornton, however, uses the value evaluated by Lee of $\alpha = \beta = 0.729$ and uses equation (2) even though L_φ and L_T are comparable. Doing this, we find that L_φ decreases from 0.56 to 0.26 μm with $L_\varphi = 0.36$ μm at $T = 19$ K. These latter values are consistent with the WL effect being one-dimensional and also with the description of the skipping orbit effect presented later.

At low temperatures, the phase breaking rate, τ_φ^{-1}, is determined by electron–electron scattering and for a one-dimensional channel is given by [11, 12]

$$\tau_\varphi^{-1} = \frac{\pi}{2}\frac{(k_B T)^2}{\hbar E_F}\ln\left(\frac{E_F}{k_B T}\right) \qquad \text{for } T > \frac{\hbar}{k_B \tau_c} \tag{5a}$$

and

$$\tau_\varphi^{-1} = \left(\frac{k_B T}{D^{1/2} W N_0 \hbar^2}\right)^{2/3} \qquad \text{for } T < \frac{\hbar}{k_B \tau_c} \tag{5b}$$

where k_B is the Boltzmann constant, E_F is the Fermi energy and N_0 is the density of states. These one-dimensional equations are valid provided $W < \pi L_T$, which is true over the temperature range considered (for $T > 38$ K, the UCF are too small to be analysed). For this channel, $\hbar/k_B\tau_c \simeq 14$ K, indicating that both terms are important in our temperature range. In figure 3, values of L_φ obtained from the UCF are plotted against temperature. The lines represent (5*a*) and the combined rate of (5*a*) and (5*b*), using values for E_F, D and W obtained from calculations described later. Note also that the two-dimensional density of states $N_0 = m^*/\pi\hbar^2$ is used (see section 2). Similar fits, using values of L_φ consistent with those in figure 3, are obtained by Choi *et al* [12] for a comparable sample ($W = 0.21\ \mu$m).

3.2. Electron interaction effects

The background magnetoresistance of the traces shown in figure 2 can be explained by considering two electronic processes. First, consider electron–electron interaction effects. Choi *et al* [3] have shown that, for narrow channels in GaAs/(AlGa)As heterostructures, the correction to the Drude conductivity of a 2D electron system is given by [13]

$$\delta\sigma = -\frac{e^2 g_{2D}}{2\pi^2\hbar}\left[\psi\left(0.5 + \frac{\hbar}{k_B T\tau}\right) - \psi(0.5)\right] \tag{6}$$

where ψ is the digamma function. As described by Choi, there is some confusion as to whether τ should be equated to τ_c or τ_t. The term g_{2D} is the interaction parameter and is given by

$$g_{2D} = 4 - 3\left(\frac{2+F}{F}\right)\ln[1 + F/2]. \tag{7}$$

F is the direct Coulomb interaction parameter and its expected value for our system is 0.45 [3, 14]. The resistivity correction can be obtained by the inversion of the conductivity tensor [15]

$$\delta\rho(B) = -\left(\frac{1-(\omega_c\tau_c)^2}{\sigma_0^2}\right)\delta\sigma \tag{8}$$

where $\omega_c = eB/m^*$. Hence

$$\Delta\rho(B) = \delta\rho(B) - \delta\rho(0) = -\frac{g'_{2D}}{2\pi^2\hbar n_s^2}\left[\psi\left(0.5 + \frac{\hbar}{k_B T\tau}\right) - \psi(0.5)\right]B^2 \tag{9}$$

where $g'_{2D} = (\tau_c/\tau_t)^2 g_{2D}$.

The Zeeman effect also affects electron interaction, although it only becomes important when $B > (k_B T/g^*\mu_B) = 12$ T where μ_B is the Bohr magneton and g^*, the effective electron g-factor, has the value 0.52 [16].

With regard to electron interaction, the cross-over to a one-dimensional effect is usually defined by [17]

$$W < \pi(\hbar D/k_B T)^{1/2} = \pi L_T. \tag{10}$$

For a one-dimensional channel, the correction is given by

$$\Delta\rho(B) = -\frac{g'_{1D}}{n_s^2\sqrt{2}\pi\hbar W}\left(\frac{\hbar D}{k_B T}\right)^{1/2} B^2 \tag{11}$$

where $g'_{1D} = (\tau_c/\tau_t)^2 g_{1D}$ and

$$g_{1D} = \frac{4.91}{\pi}\left[1 - 12\left(\frac{1 + F/4 - (1+F/2)^{1/2}}{F}\right)\right]. \tag{12}$$

If $\tau_c < \tau_t$ then the interaction effects are said to be 'suppressed' because $g' < g$.

It is found that, for traces below 48 K, the data in the B-field range 0–0.74 T can only be fitted to the suppressed one-dimensional interaction equation. Consider the values of the parameters used in equation (11). n_s was obtained from Shubnikov–de Haas (SDH) analysis (see later). Since the suppression indicates a specular side-wall scattering process, this scattering does not alter the electron momentum along the channel and hence the diffusion coefficient is given by

$$D = v_F^2 \tau_t / 2. \tag{13}$$

The value of τ_t can be obtained from the Drude conductance and is proportional to W^{-1}. Therefore, using equations (11), (13) and $\Delta R(B) = \Delta\rho(B)L/W$, the unknown parameter, used as the adjustable parameter in the fitting process, is $W^{-5/2}(\tau_c/\tau_t)^2$. If we assume $W = 0.34 \pm 0.02\ \mu$m, consistent with later results, we obtain $\tau_t/\tau_c = 2.4 \pm 0.3$. Similar ratios, also explained in terms of a specular side-wall scattering process, have been observed by Choi *et al* [3]. If we use $W = 0.34 \pm 0.02\ \mu$m then we obtain $\tau_t = (1.3 \pm 0.1) \times 10^{-12}$ s from the Drude conductance.

τ_c and τ_t could also differ due to the presence of electron–electron inelastic scattering where the momentum is merely redistributed amongst the electrons rather than altering the conduction along the channel. Hence τ_φ^{-1} would not affect τ_t^{-1} but could alter τ_c^{-1}. However, using the values of τ_φ obtained in § 3.1 we would expect τ_t/τ_c to change from 1.2 to 2.4 between 4.2 and 38 K. This does not agree with the observed temperature independent value of 2.4 ± 0.3. This temperature independence is consistent with the presence of specular side-wall scattering.

Neither the suppressed one-dimensional nor the suppressed two-dimensional equation can fit the trace at the next temperature ($T = 48$ K). However, the unsuppressed 2D equation gives a fit within the allowed errors. Here again n_s, F and W are used as known parameters and from this $\tau_t = (1.3 \pm 0.2) \times 10^{-12}$ s is obtained, in agreement with the above value. The use of the *un*suppressed equation is consistent with the picture presented, since if the system is two-dimensional in respect to electron interaction effects, the presence of the side walls and the specular scattering will not influence the electronic motion. Therefore $\tau_c = \tau_t$ is used in equation (9).

Using (10), a dimensional crossover between $T = 38$ K and 48 K suggests a channel width of 0.33–0.38 μm, which is close to the physical width of 0.32 μm. Analysis at higher temperatures is prevented by the presence of a positive magnetoresistance term which can be explained in terms of non-degenerate effects (see below).

3.3. *Classical magnetoresistance effects*

Classically, if τ_c is assumed to be energy independent then $\rho_{xx} = \sigma_0^{-1}$ and $\rho_{xy} \simeq B r_H / n_s e$ (where x and y are the channel length and width directions, r_H is the Hall factor). Hence there is no magnetoresistance along the channel [18]. For a degenerate 2DEG, only the electrons close to the Fermi energy are capable of being scattered. Therefore τ_c is constant and the above equations are valid. However, for traces above $T = 48$ K a positive magnetoresistance proportional to B^2 is clearly seen. At these higher temperatures the 2DEG is no longer sufficiently degenerate and the temperature dependence of τ_c has to be considered [18].

Boundary scattering alters the behaviour described by the above equations. Figure 4 shows the 9.2 K magnetoresistance trace plotted against B^2. The fit shown in the region above the field value $B_s = 0.74$ T is to equation (11). However, below B_s there is clearly an additional component to the background negative magnetoresistance. This

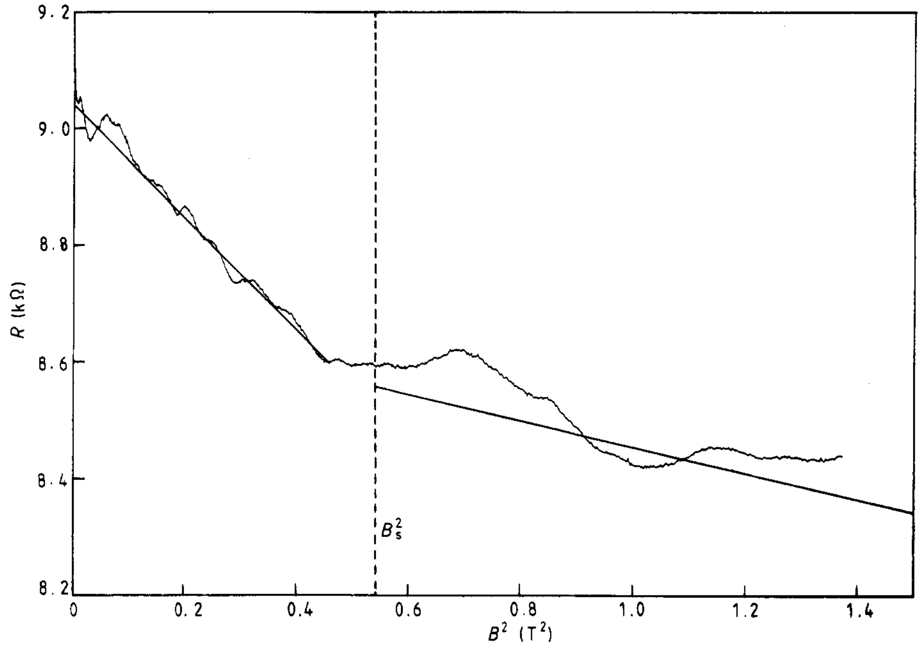

Figure 4. The magnetoresistance of the 9.2 K trace plotted against B^2. The straight lines are predictions based on the presence of a specular side-wall scattering process (see text for details).

magnetoconductivity enhancement, first observed by Choi *et al* [3], can be explained in terms of a skipping orbit formation due to the presence of specular side-wall scattering. The same effect is not achieved with diffuse side-wall scattering. Although an exact theory has not been developed for this effect, the magnetoresistance is frequently assumed to fall off as B^2 until saturation occurs. This saturation will occur at magnetic field values large enough for electrons to complete cyclotron orbits without hitting the side walls. A channel width of $(3.4 \pm 0.2) \times 10^{-7}$ m is obtained from B_s, which is temperature independent as expected, by using the equation

$$W = 21_{\text{cyc}} = 2m^* v_F / eB_s. \tag{14}$$

By extrapolating the interaction fit line below B_s in figure 4, the net gradient G for this skipping effect can be obtained. We define $G = G_1 - G_2$ where G_2 is the gradient of the fit to the data below B_s and G_1 is the gradient of the interaction fit line. Figure 5 shows the temperature variation of G. The almost temperature-independent behaviour of G seen below 20 K is consistent with that observed by others [3, 19] at similar temperatures. However, the effect develops a significant temperature dependence at higher temperatures, a result which, to our knowledge, has not been studied elsewhere. The magnitude of G reflects the strength of the skipping orbit process, which is limited by the rate at which electrons scatter out of the orbits. Collisions with short range scatterers within the channel and inelastic collisions (with rates τ_t^{-1} and τ_φ^{-1} respectively) will both limit G. The fits to equations (9) and (11) confirm that τ_t is temperature independent up to at least 48 K, whilst analysis of the UCF shows that τ_φ has a temperature dependence given by equation (5). Hence the trends seen in figure 5 can be explained as follows.

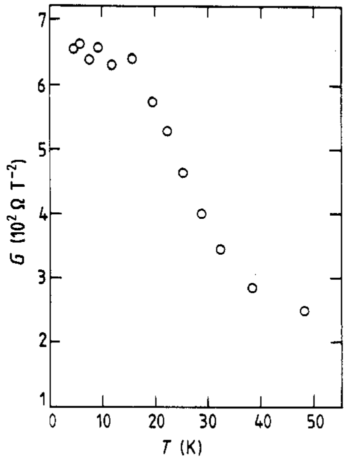

Figure 5. The net gradient G plotted against temperature T.

Below 20 K the temperature-independent elastic scattering rate determines G. Previous results indicate that above 20 K, $\tau_\varphi < \tau_t$ and so τ_φ^{-1} should dominate the scattering rate. Above 20 K, the fall-off with temperature of G is proportional to the rate τ_φ^{-1} suggested by equation (5).

The above cyclotron effect is a classical one. In systems where the electron mobilities are higher, and hence SDH oscillations persist to smaller fields B, the effect of side-wall confinement on the quantum mechanical picture can be studied and has been the subject of a great deal of recent interest [20, 21].

Summarising, the low field magnetoresistance of a 0.32 μm structure has been fully explained in terms of three electronic transport phenomena. Below 48 K the channel is one-dimensional with respect to electron interaction effects. The interaction is suppressed due to the presence of specular side-wall scattering which results in a ratio $\tau_c/\tau_t \simeq 2.4 \pm 0.3$. This side-wall scattering also results in an extra negative magnetoresistance component below $B_s = 0.74$ T, which is due to the formation of skipping orbits along the side walls. Both the skipping orbit and the electron interaction magnetoresistances reveal that the conducting and physical channel widths are comparable. This is in sharp contrast to the results of other workers (e.g. [5, 19]) who find that the conducting width is much smaller. At temperatures below 20 K, the skipping orbit effect is temperature independent, as seen by others [5, 19]. However, at higher temperatures we observe a reduction of this process which can be explained in terms of the size and temperature dependence of τ_φ as obtained from the analysis of the UCF.

4. Time-dependent instabilities

Magnetoresistance measurements made on a channel of physical width 0.54 μm are shown in figure 6. The traces, recorded at 4.2 K, demonstrate the effect of rotating the magnetic field, with the horizontal axis corresponding to $B \cos \theta$, where θ is the angle between B and the normal to the 2DEG plane. We briefly reported these results in a previous article [22]. Similar behaviour has been reported by Kaplan and Harstein [6] for Si MOSFETS although in their case the scaling of the magnetoresistance with cos θ was not as clear. Since the three conduction processes outlined in § 3 are sensitive to the

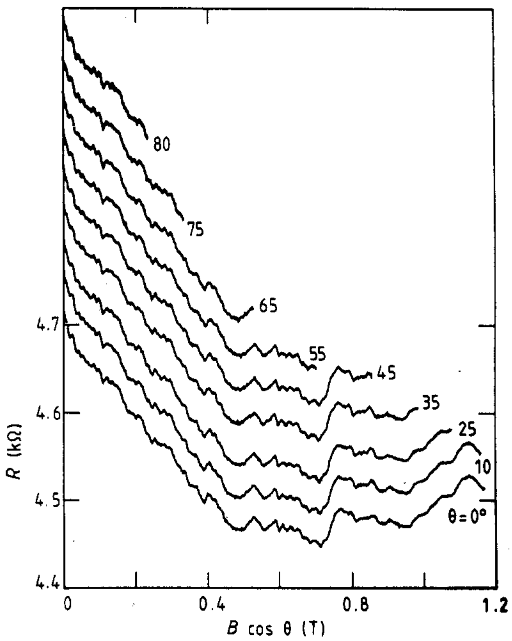

Figure 6. Transverse magnetoresistance of a 0.54 μm wide structure at 4.2 K plotted against $B \cos \theta$ for various angles of θ (the angle between $\boldsymbol{B}$ and the normal of the 2DEG plane). The traces for $\theta \geqslant 10°$ are offset vertically.

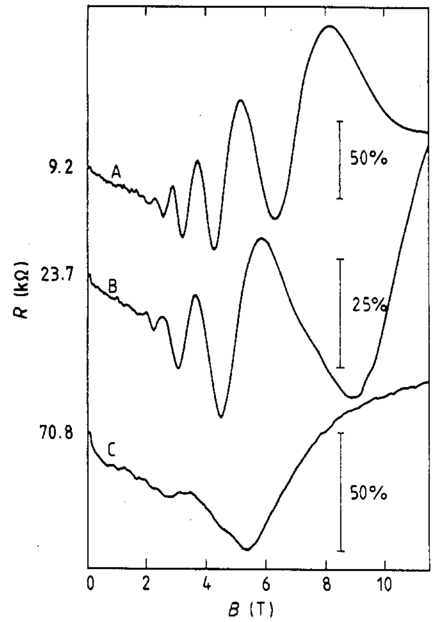

Figure 7. Magnetoresistance of three different 'states' of the structure with a lithographic width of 0.32 μm and carrier concentrations (A) 6.1, (B) 4.3 and (C) 2.6×10^{11} cm^{-2}. The percentage resistance markers are relative to the zero-field resistances for each trace.

component of the field B perpendicular to the electron trajectories, this exact scaling with $\cos \theta$ shows that the electronic motion is indeed confined to a two-dimensional plane. The positive magnetoresistance seen above 0.5 T is a result of non-degenerate effects and becomes more pronounced at higher temperatures, so preventing the analysis described in § 3. However, as with the 0.32 μm channel, the physical and conducting channel widths are expected to be comparable.

The traces shown in figures 2 and 6 are for the most stable 'states' observed for the two channels. If the structures are left at helium temperatures, the channels deteriorate in discrete steps, each step characterised by a fall in n_s (obtained from SDH analysis) and a rise in the Drude resistance R. This instability increases for narrower channels and also a 'bulk' 2DEG ($W = 0.16$ mm) shows no change of state, suggesting that the deterioration is associated with the confining side walls.

Several of the states experienced by the 0.32 μm channel over a three-day period are shown in figure 7. The small aperiodic oscillations seen below 2 T are the UCF. The larger oscillations seen above 2 T, which are periodic in B^{-1}, are SDH oscillations. At high B-fields, where the SDH oscillations are more established, the UCF disappear since the electrons move in tight Landau orbits and are not able to complete the loops necessary for quantum interference effects. The magnetic field B_c at which this observed quenching of the UCF occurs is dictated by the comparative sizes of the impurity separation length L_e, which determines the minimum size of the QI loops, and the Nth-Landau-level orbit

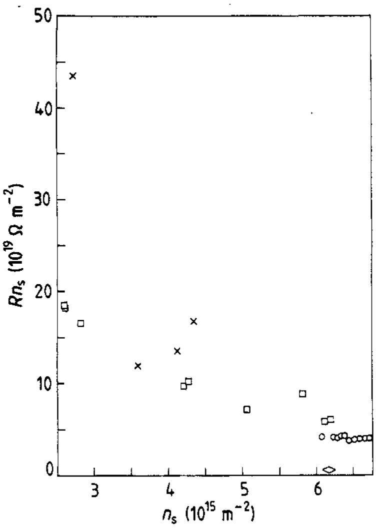

Figure 8. The product Rn_s plotted against n_s for various states of structures with lithographic widths of 0.18 μm (crosses), 0.32 μm (squares), 0.54 μm (circles) and 160 μm (diamond).

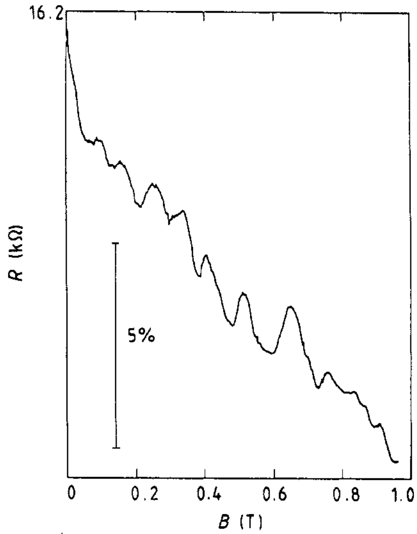

Figure 9. Low field magnetoresistance of a 0.32 μm wide structure, showing a dominance of a single frequency in the UCF spectrum. The 5% marker is relative to the zero-field resistance R = 16.2 kΩ. T = 4.2 K.

diameter $d = 2[(2N_L + 1)(\hbar/eB)]^{1/2}$. For all the 'states' where L_e is known (see later), it is found that $d < L_e$ is true for all N_L such that $B > B_c$.

In figure 8 the product n_sR is plotted against n_s for each of the states monitored. Since, for a uniform n_s and μ, the product is given by

$$n_sR = L/e\mu W \tag{15}$$

the trend shows that, as n_s decreases, there is also a reduction in the product μW. An independent method of monitoring μ is needed to see which of the two parameters, μ and W, is changing. We do this by considering the UCF spectrum. Using the physical interpretation of the UCF phenomenon described earlier, it is possible to relate the period ΔB (in T) of a particular fluctuation to the area A of the scattering loop within the channel by $A = h/e\Delta B$. For certain states one frequency dominates the UCF spectrum. An example trace is shown in figure 9. This frequency can be attributed to the loop trajectory with the smallest perimeter, since the probability of phase coherence between the partial waves is highest and hence the interference process will be strongest. The smallest loop possible is one involving three impurity scattering sites only (note that for loops featuring a side-wall scattering event there is a larger range of possible enclosed areas and these therefore would not produce the definite period seen in figure 9). Taking the loop geometry to be that of a triangle, it is possible to relate this dominant frequency to the area and hence the side length, L_e, of the triangle. Thus for each state revealing a dominant period, the impurity separation length L_e and the corresponding time $\tau_e = L_e/v_F$ are known. The identification of the smallest loop with a triangle is not strictly necessary. All we assume is that the area of the loop is proportional to L_e^2. At 4.2 K for the most stable state the value of τ_e obtained in this manner is equal to the value of τ_t obtained from the 2D electron interaction equation. Assuming this equality holds for the

Table 2. Various parameters describing six 'states' of the 0.32 μm wide structure observed at 4.2 K (see text for details).

State	R ($\pm$0.01) (kΩ)	n_s ($\pm$0.1) (10^{15} m^{-2})	v_F ($\pm$0.03) (10^5 m s^{-1})	L_e ($\pm$0.01) (μm)	μ ($\pm$0.1) (m^2 V^{-1} s^{-1})	W ($\pm$0.03) (μm)	$\tau_\varphi = L_\varphi^2/D$ ($\pm$1) (10^{-12} s)
1	9.30	6.2	3.37	—	—	—	—
2	13.86	5.8	3.16	0.32	2.0	0.33	2
3	16.50	5.2	2.98	0.31	1.9	0.29	2
4	23.70	4.3	2.71	0.28	1.9	0.25	2
5	58.50	2.8	2.20	0.14	1.3	0.22	4
6	70.80	2.6	2.10	0.14	1.4	0.21	—

other less stable states we determine τ_e from the dominant UCF period and hence τ_t for each of them. The value of μ obtained from τ_t can then be used to extract an approximate value of W from equation (15).

Table 2 shows parameters describing six 'states' for a channel with a physical width of 0.32 μm. The Fermi energy, and hence the Fermi velocity v_F, is calculated from n_s using the 2D density of states equation. L_e, μ and W are obtained as described above. The values of W are consistent with the results of the previous section, where 'state 1' was shown to have an approximate width of 0.34 ± 0.03 μm. The decrease in n_s is accompanied by a reduction in W and $\tau_e = L_e/v_F$. Further measurements are necessary before an exact relationship between n_s and τ_e can be established.

The value of L_φ is calculated from the UCF amplitude. It is not clear how L_φ and τ_φ should be related. Since τ_φ and τ_t are of a similar size, the motion along the channel is not truly diffusive ($\tau_\varphi = L_\varphi^2/D$) nor is it ballistic ($\tau_\varphi = L_\varphi/v_F$). For the results shown in § 3.1 and table 2 the diffusive relationship was used. However, using either equation, τ_φ is found to be constant within error as n_s decreases.

Finally, in addition to the above effect, some channels reveal another type of time dependent instability, where the resistance switches between two discrete values. This effect, similar to the 'telegraph noise' observed by Skocpol *et al* [23] and others, is attributed to a single electron being captured by a trap. The capture of the electron is thought to change the potential in the channel and hence produce a small change in conductivity.

5. Conclusions

We have analysed magnetoresistance measurements in terms of electronic conduction in the quasi-ballistic regime, including the effect of boundary scattering. In particular, we have observed a temperature dependent classical magnetoresistance effect involving the formation of skipping orbits along the confining side walls. The presence of these orbits, and the ratio $\tau_t/\tau_c \simeq 2.4 \pm 0.3$, suggest that the boundary scattering is predominantly specular. This is as expected since the nature of this scattering depends on the ratio of λ_F to the surface roughness. For these channels the electron density gives a much larger Fermi wavelength than in metals ($\lambda_F = 30$ nm) and the confining potential is expected to be smooth since the 2DEG layer was not etched, so reducing surface damage.

The specular nature of the side-wall scattering and the comparable sizes of the physical and conduction channel make the shallow etch confinement technique a potentially useful one. However, channels confined in this way were found not to be stable at helium temperatures. The depletion of carriers was accompanied by a reduction in channel width and the mobility. Since the instability was greatest for the narrower channels and also n_s decreased with width, the degradation is assumed to be a side-wall effect.

References

[1] Thoms S, McIntrye I, Beaumont S P, Al-Mudares M, Cheung R and Wilkinson C D W 1988 *J. Vac. Sci. Technol.* B **6** 127

[2] Reviews by
Lee P A and Ramakrishan T V 1985 Disordered electronic systems *Rev. Mod. Phys.* **57** 287–337
Al'tushuler B L and Aronov A G 1985 *Electron–Electron Interactions in Disordered Systems* ed. A L Efros and M Pollak (Amsterdam: North Holland) p 1
Lee P A, Stone A D and Fukuyama H 1985 *Phys. Rev.* B **35** 1039

[3] Choi K K, Tsui D C and Palmateer S C 1985 *Phys. Rev.* B **32** 5540; 1986 *Phys. Rev.* B **33** 8216

[4] Lakrimi M, Grassie A D C, Hutchings K M, Harris J J and Foxon C T 1990 Scattering change in GaAs–(AlGa)As heterojunctions *Semicond. Sci. Technol.* submitted

[5] Thornton T J, Pepper M, Ahmed H, Andrews D and Davies G J 1986 *Phys. Rev. Lett.* **56** 1198; 1987 *Phys. Rev.* B **36** 4514

[6] Kaplan S B and Harstein A 1986 *Phys. Rev. Lett.* **56** 2403

[7] Das Sarma S and Stern F 1985 *Phys. Rev.* B **32** 8442

[8] Van Houten H, Van Wess B J and Beenakker C W J 1988 *Springer Series in Solid State Sciences* vol 83 (Berlin: Springer) p 198

[9] Lee P A, Stone A D and Fukuyama H 1987 *Phys. Rev.* B **35** 1039

[10] Beenakker C W J and Van Houten H 1988 *Phys. Rev.* B **37** 6544

[11] Dynes R C 1982 *Physica* B **109 + 110** 1857

[12] Choi K K, Tsui D C and Alavi K 1987 *Phys. Rev.* B **36** 7751

[13] Fukuyama H J 1981 *J. Phys. Soc. Japan* **50** 3407

[14] Altshuler B L, Aronov A G and Lee P A 1980 *Phys. Rev. Lett.* **44** 1288

[15] Houghton A, Senna J R and Ying S C 1982 *Phys. Rev.* B **25** 2196

[16] Englert Th, Tsui D C, Gossard A C and Uihlei Ch 1982 *Surf. Sci.* **113** 295

[17] Altshuler B L, Khmel'nitzkii D, Larkin A I and Lee P A 1980 *Phys. Rev.* B **22** 5142

[18] Seeger K 1982 *Semiconductor Physics* (New York: Springer)

[19] Van Houten H, Beenakker C W J, Broekaant M E I, Heijman M G J, Van Wees B J, Mooij J E and Andre J P 1988 *Acta Electronica* **28** 27

[20] Wharam D A, Thornton T J, Newbury R and Pepper M 1988 *J. Phys. C: Solid State Phys.* **21** 209–14

[21] Van Wees B J, Kouwenhoven L P, Van Houten M, Beenakker C W J, Mooij J E, Foxon C T and Harris J J 1988 *Phys. Rev.* B **38** 3625–7

[22] Taylor R P, Leadbeater M L, Whittington G P, Main P C, Eaves L, Beaumont S P, McIntyre I, Thoms S and Wilkinson C D W 1988 *Proc. 7th Conf. Electronic Properties of Two Dimensional Systems; Surf. Sci.* **196** 52–8
See also
Main P C, Eaves L, Taylor R P, Whittington G P, Thoms S, Beaumont S P and Wilkinson C D W 1986 *Proc. 18th Int. Conf. Physics of Semiconductors, Stockholm, 1986* (Singapore: World Scientific) p 1591

[23] Skocpol W J, Mankiewich P M, Howard R E, Jackel L D, Tennant D M and Stone A D 1986 *Phys. Rev. Lett.* **56** 2865